× 5 - 2 × 8), as found in this complex and in many carbonyl cluster compounds.[22] Though the square-pyramidal clusters with π-acceptor ligands usually have 74 electrons, those with π-donor ligands may have a smaller number of electrons due to the destabilization of the valence-shell d orbitals by the repulsion with π-electrons of the ligands. For example, a square-pyramidal cluster, $[Mo_5Cl_{13}]^-$, has only 68 electrons.[23] The existence of complexes **1** and **2** shows that the square-pyramidal cluster can achieve the upper limit of electrons even with π-donor ligands. As the relationship between the cluster shape and the number of valence electrons in the present class of sulfido clusters is interesting, we are currently preparing other metal derivatives.

Acknowledgment. The support from the Ministry of Education, Science, and Culture of Japan (Grant-in-Aid for Scientific Research No. 63430010) and the gift of triethylphosphine from Nippon Chemical Co. Ltd. are gratefully acknowledged.

Supplementary Material Available: Listings of detailed crystal data, positional parameters for hydrogen atoms, anisotropic thermal parameters, and bond distances and angles for non-hydrogen atoms (7 pages); a Table of calculated and observed structure factors (38 pages). Ordering information is given on any current masthead page.

(22) (a) Lauher, J. W. *J. Am. Chem. Soc.* **1978**, *100*, 5305. (b) Teo, B. K. *Inorg. Chem.* **1985**, *24*, 1627. (c) Johnston, R. L.; Mingos, D. M. P. *Inorg. Chem.* **1986**, *25*, 1661.
(23) Jödden, K.; von Schnering, H. G.; Schäfer, H. *Angew. Chem., Int. Ed. Engl.* **1975**, *14*, 570.

Contribution from the Department of Inorganic and Analytical Chemistry, Universität-GH Paderborn, 4790 Paderborn, FRG

Deprotonation of $Re_2(\mu\text{-}H)(\mu\text{-}PPh_2)(CO)_8$ for Synthesis of Mixed Rhenium-Gold Clusters with Re_2Au_n Cores (n = 1-3)

H.-J. Haupt,* C. Heinekamp, and U. Flörke

Received November 9, 1989

The dirhenium complex $Re_2(\mu\text{-}H)(\mu\text{-}PPh_2)(CO)_8$ (**1**) is deprotonated with NaOEt (or 1,8-diazabicyclo[5.4.0]undec-7-ene, DBU) to give the anion $[(\mu\text{-}PPh_2)(CO)_8Re_2]^-$ (**2**$^-$), which was isolated as tetraethylammonium salt $[C_8H_{20}N]$[**2**]. The exchange of the isolobal fragment $AuPPh_3$ for H in **1** (via **2**$^-$) generates $[(\mu\text{-}PPh_2(CO)_8Re_2AuPPh_3]$ (**3**). The treatment of **1** in THF solution with lithium organyls RLi (R = Me, *n*-Bu, Ph) gives products of two types: first, $[(\mu\text{-}C(R)O)(\mu\text{-}PPh_2)(CO)_6Re_2(AuPPh_3)_2]$ (R = Ph (**4**), Me (**5**), *n*-Bu (**6**)) and, second, $[(\mu\text{-}PPh_2)(CO)_6Re_2(AuPPh_3)_3]$ (**7**). Complex **1** was also reacted with diphenylacetylene to give $[(\mu\text{-}\sigma\text{:}\eta^2\text{-}CPh{=}CHPh)(\mu\text{-}PPh_2)(CO)_7Re_2]$ (**8**). ^{31}P NMR data have been measured for the newly synthesized compounds. The molecular structures of $[C_8H_{20}N]$[**2**], **3**, **4**, **7**, and **8** have been determined from X-ray data collected on an automated diffractometer with monochromatized Mo Kα radiation. Compounds **3**, **7**, and **8** crystallize in the triclinic space group $P\bar{1}$ with Z = 2, while **2** and **4** crystallize in the monoclinic space groups $C2/c$ with Z = 8 and $P2_1/n$ with Z = 4, respectively. For **2**, a = 18.007 (3) Å, b = 17.165 (3) Å, c = 21.368 (5) Å, and β = 109.36 (1)°; for **3**, a = 14.918 (7) Å, b = 15.456 (4) Å, c = 9.229 (4) Å, α = 93.12 (1)°, β = 97.10 (1)°, and γ = 83.27 (1)°; for **4**, a = 24.434 (4) Å, b = 10.284 (2) Å, c = 24.618 (4) Å, and β = 113.75 (1)°; for **7**, a = 13.676 (5) Å, b = 13.817 (4) Å, c = 21.723 (7) Å, α = 71.26 (1)°, β = 87.05 (1)°, and γ = 82.37 (1)°; and for **8**, a = 9.436 (2) Å, b = 11.774 (3) Å, c = 14.353 (4) Å, α = 95.91 (2)°, β = 99.57 (2)°, and γ = 95.71 (2)°. The molecular structure of the diamagnetic anion **2**$^-$ as the $[NEt_4^+]$ salt contains an $Re_2(\mu\text{-}P)$ ring with four cis-terminal carbonyl ligands at each Re atom of an idealized C_{2v} symmetry. The Re-Re bond length is 3.062 (2) Å with bond angle Re-P-Re = 78.6 (1)°. The addition of the sterically demanding $[AuPPh_3^+]$ cation to **2**$^-$ leads to a planar four-membered $AuPRe_2$ ring in **3**. The Re-Re bond of 3.225 (2) Å is elongated and the angle Re-P-Re = 83.8 (3)° enlarged compared to those of $[C_8H_{20}N]$[**2**]. The average Au-Re single-bond length is 2.787 (2) Å. The molecular structure of **4** shows an Re_2Au_2 metallatetrahedron core in which the Re-Re bond is bridged through the acylic C(Ph)O group (Re-C = 2.17 (3) Å, C-O = 1.24 (4) Å). The Re-Re bond length is 3.122 (2) Å, and the other metal-metal distances are 2.734 (2) Å (Au-Au) and 2.901 (2) Å (average Au-Re). These values are consistent with metal-metal single bonds. The molecular structure of **7** contains a trigonal-bipyramidal Re_2Au_3 core. The Re-Re bond length of 2.914 (3) Å, of double-bond character, is shorter than that of **4**, whereas the average Au-Au bond length of 2.829 (2) Å is elongated; the average Au-Re bond length is 2.830 (2) Å. The molecular structure of **8**, which results from a release of one CO ligand from **1** and a hydride transfer to coordinated diphenylacetylene, contains the vinylic $\mu\text{-}\sigma\text{:}\eta^2$-CPh=CHPh ligand (C=C = 1.394 (16) Å) bridging an Re-Re bond, Re-Re = 2.998 (1) Å. In the isoelectronic series of compounds **1**-**3** in which the H^+ in **1** is substituted by the isolobal fragment $[PPh_3Au^+]$ via the anion **2**$^-$, the Re_2 core becomes more electron-rich, which facilitates the anodic one-electron transfer as measured by cyclic voltammetry; i.e., $E_{p,a1}$ decreases from 1508 mV in **1** to 1132 mV in $[C_8H_{20}N]$[**2**] to 241 mV in **3**. The same is observed for the Re_2 core in the exchange of an electron-poor phenyl acyl against an electron-rich diisopropylamino acyl group in the isoelectronic compounds of the type $[(\mu\text{-}C(R)O)(\mu\text{-}PPh_2)(CO)_6Re_2(AuPPh_3)_2]$ (R = Ph, E^f = 682 mV; R = N(*i*-Pr$_2$), E^f = 576 mV). For **7** the E^f values of the reversible one-electron-transfer processes are 289 and 752 mV.

Introduction

This study continues our recent work on the reactions between dirhenium decacarbonyl and diphenylphosphine at different molar ratios, which have yielded $Re_2(\mu\text{-}H)(\mu\text{-}PPh_2)(CO)_8$[1] (**1**) and $Re_2(\mu\text{-}PPh_2)_2(CO)_8$.[2] We describe now the deprotonation of the hydrido-bridged compound **1** with different bases such as sodium ethanolate, 1,8-diazabicyclo[5.4.0]undec-7-ene (DBU), and especially nucleophiles R$^-$ in LiR (R = Me, *n*-Bu, Ph). Anionic intermediates have been isolated and identified as well as different dirhenium gold clusters obtained from the reaction of the anionic intermediates with PPh_3AuCl. It might be anticipated from the isolobal relationship of H with $AuPPh_3$[3] that the basic property of such reagents possibly generates via the intermediate $[(\mu\text{-}PPh_2)(CO)_8Re_2]^-$ (**2**$^-$) the substance $[(\mu\text{-}PPh_2)(CO)_8Re_2AuPPh_3]$ (**3**). By contrast, the assumption of gold atom uptake in the reaction of PPh_3AuCl with anionic intermediates obtained in the reaction of **1** with RLi followed by release of RH and acylation of coordinated carbonyls cannot reasonably be made without related experiments. It can only be said that the intented auration of **1** may be limited as the consequence of a reduced capability of C atoms in CO ligands to be converted into acyl fragments. Each acylation process then produces a higher electron density

(1) Haupt, H. J.; Balsaa, P.; Flörke, U. *Inorg. Chem.* **1988**, *27*, 280; *Z. Anorg. Allg. Chem.* **1987**, *548*, 151.
(2) Flörke, U.; Woyciechowski, M.; Haupt, H. J. *Acta Crystallogr., Sect. C: Struct. Crystallogr., Cryst. Chem.* **1988**, *C44*, 2101.
(3) (a) Evans, D. G.; Mingos, D. M. P. *J. Organomet. Chem.* **1982**, *232*, 171. (b) Johnson, B. F. G.; Lewis, J.; Nicholls, N.; Puga, J.; Whitmire, K. H. *J. Chem. Soc., Dalton Trans.* **1983**, 787. (c) Stone, F. G. A. *Angew. Chem., Int. Ed. Engl.* **1984**, *23*, 89 and references cited therein.

0020-1669/90/1329-2955$02.50/0

in the remaining CO ligands, which lowers their affinity for a further nucleophilic attack by R^-. The new substances **2**$^-$–**4** and **7** obtained from such examinations have been identified by single-crystal X-ray analysis, and derivatives were characterized by means of $^{31}P\{H\}$ NMR data. Redox properties were determined by cyclic voltammetric measurements. Such heterobimetallic compounds with a transition metal and a coinage metal, especially gold, are presently of interest both due to their potential as homogeneous catalysts and for theoretical considerations.[4,5]

Apart from this, the reactivity of the μ-H atom in **1** was characterized through its reaction with diphenylacetylene, giving $Re_2(CO)_7(\mu\text{-}\sigma\text{:}\eta^2\text{-}CHPhCHPh)(\mu\text{-}PPh_2)$ (**8**).

Experimental Section

The reactions were performed under an argon atmosphere in deoxygenated solvents that were dried by standard methods.

Materials. $Re_2(CO)_8(\mu\text{-}H)(\mu\text{-}PPh_2)$ was prepared according to the literatue method.[1] $Re_2(CO)_{10}$ and PPh_3AuCl were purchased from Strem Chemicals.

Preparation of $[C_8H_{20}N][2]$. A 30-mL ethanolic solution of **1** (0.2 g; 0.26 mmol) and NaOEt (34.3 mg; 0.5 mmol) was heated 4 h under reflux of the solvent. Afterward, Et_4NCl was added to the yellow solution to get the related ammonium salt of the before-formed dirhenium anion. For separation of this salt the solvent EtOH was vacuum-stripped to leave an air-stable solid. The salt was extracted from this residue by use of acetone and crystallized from the eluant as yellow $[Et_4N][(\mu\text{-}PPh_2)(CO)_8Re_2]$ (54 mg; 24%). Single crystals of $[C_8H_{20}][2]$ were generated through an application of the vapor diffusion equalization method with CH_2Cl_2/pentane. Anal. Calcd for $C_{28}H_{30}O_8PNRe_2$: C, 36.85; H, 3.29; N, 1.54. Found: C, 36.40; H, 3.49; N, 1.82. IR frequencies (cm^{-1}) (CH_2Cl_2): ν(C≡O) 2078 vw, 2040 w, 1990 vs, 1942 vs, 1878 sh.

Preparation of 3. To a 20-mL THF solution of **1** (0.2 g; 0.26 mmol) was added 50 μL (0.28 mmol) of DBU at room temperature. The yellow solution was stirred for 1 h, and then PPh_3AuCl (124 mg; 0.25 mmol) was added. Afterward, the mixture was cooled to −30 °C and filtered to remove the precipitate of DBU hydrochloride. The THF filtrate was evaporated to dryness, and from CH_2Cl_2 solution of the residual solid the desired product was crystallized by use of the vapor diffusion method (CH_2Cl_2/*n*-pentane). Yield: 176 mg (52%). Anal. Calcd for $C_{38}H_{25}O_8P_2AuRe_2{\cdot}CH_2Cl_2$: C, 35.30; H, 2.04. Found: C, 35.40; H, 2.98. IR frequencies (cm^{-1}) (CH_2Cl_2): ν(C≡O) 2040 m, 1985 vs, 1950 vs, 1913 s.

Preparation of $[(\mu\text{-}C(R)O)(\mu\text{-}PPh_2)(CO)_6Re_2(AuPPh_3)_2]$ with R = Ph (4), Me (5), and *n*-Bu (6). To each 20-mL THF solution of **1** (0.2 g; 0.26 mmol) was added the appropriate LiR reagent (R = Ph, 0.59 mmol; R = Me and *n*-Bu, 0.54 mmol) at −78 °C. The orange solutions were always cooled for 1 h. In each experiment the solution was then allowed to warm to room temperature before adding PPh_3AuCl (248 mg; 0.5 mmol). All three reaction mixtures were stirred afterward for 1 h. For the subsequent product separation, the solvent was vacuum-stripped to leave a colored air-stable solid. The components of each residue were obtained by use of the TLC separation procedure (PSC plate, silica 60, Fa. Merck) with CH_2Cl_2/*n*-hexane as eluant. In the case of **4**, the chromatogram contained one orange main fraction. From a CH_2Cl_2 solution of the fraction were obtained two components, crystallized by the vapor diffusion method (CH_2Cl_2/*n*-pentane) as orange and dark brown substances. Their manual separation gave 136.6 mg (30.7%) of **4** and 9.3 mg (1.6%) of $(\mu\text{-}PPh_2)(CO)_6Re_2(AuPPh_3)_3$ (**7**). In the other two cases, each chromatogram was divided into a yellow and an orange region. From each region one component was dissolved in CH_2Cl_2 and crystallized by the vapor diffusion method (CH_2Cl_2/*n*-pentane). The following products, listed in order of decreasing R_f values, were identified: **5** (116.8 mg; 26.6%) and **7** (22.3 mg; 3.8%); **6** (93.8 mg; 20.8%) and **7** (5.5 mg; 0.9%).

Analytical and Spectral Data. ^{31}P NMR (Bruker WM 250) absorbance signals of the products **2**$^-$–**7** are given in Table I.

4. Mp: 189 °C dec. Anal. Calcd for **4**: C, 41.84; H, 2.57. Found: C, 41.44; H, 2.74. IR frequencies (cm^{-1}) (Perkin-Elmer Model 1330) (CH_2Cl_2): ν(C≡O) 1990 sh, 1968 vs, 1895 s.

5. Mp: 182 °C dec. Anal. Calcd for **5**: C, 39.83; H, 2.55. Found: C, 39.79; H, 2.54. ^{13}C NMR data ($CDCl_3$): δ 50.5 (s, CH_3). IR frequencies (cm^{-1}) (CH_2Cl_2): ν(C≡O) 1190 sh, 1965 vs, 1890 s.

Table I. $^{31}P\{^1H\}$ NMR Data for **2**–**7**

complex	$^{31}P\{^1H\}$ resonance, δ^a
2$^-$	89.77 (s; 1 P, μ-PPh_2)
3	119.52 (d, ^3J(PP) = 13.8 Hz; 1 P, μ-PPh_2)
	83.07 (d, ^3J(PP) = 13.8 Hz; 1 P, PPh_3)
4[b]	122.5 (dd, ^3J(PP) = 11.0, 15.7 Hz; 1 P, μ-PPh_2)
	66.5 (dd, ^3J(PP) = 11.0, 24.9 Hz; 1 P, PPh_3)
	61.1 (dd, ^3J(PP) = 15.8, 24.7 Hz; 1 P, PPh_3)
5	116.9 (dd, ^3J(PP) = 12.5, 17.7 Hz; 1 P, μ-PPh_2)
	66.4 (dd, ^3J(P) = 12.4, 26.1 Hz; 1 P, PPh_3)
	61.5 (dd, ^3J(PP) = 17.8, 26.1 Hz; 1 P, PPh_3)
6	117.8 (dd, ^3J(PP) = 12.0, 16.6 Hz; 1 P, μ-PPh_2)
	66.2 (dd, ^3J(PP) = 11.8, 25.6 Hz; 1 P, PPh_3)
	61.7 (dd, ^3J(PP) = 17.3, 25.7 Hz; 1 P, PPh_3)
7	124.0 (td, ^3J(PP) = 11.7, 11.6 Hz; 1 P, μ-PPh_2)
	73.7 (dd, ^3J(P) = 11.3, 9.9 Hz; 2 P, PPh_3)
	69.6 (td, ^3J(PP) = 10.4, 9.8 Hz; 1 P, PPh_3)

[a] Bruker WP 250 FT-NMR spectrometer; $CDCl_3$ solution at 25 °C; H_3PO_4 (85%) as standard. [b] For comparison δ values of $[(\mu\text{-}C(N(i\text{-}Pr_2))O)(\mu\text{-}PPh_2)(CO)_6Re_2(AuPPh_3)_2]$: 109.58 (m; 1 P, μ-PPh_2), 63.57 (m; 2 P, PPh_3).[17]

6. Mp: 186 °C dec. Anal. Calcd for $C_{59}H_{49}O_7P_3Au_2Re_2{\cdot}0.5CHCl_3$: C, 39.95; H, 2.79. Found: C, 40.01; H, 3.06. ^{13}C NMR data ($CDCl_3$) for *n*-Bu residue: δ 63 (s), 26 (s), 22 (s), 13 (s).

7. Mp: 190 °C dec. Anal. Calcd for $C_{72}H_{55}Re_2Au_3O_6P_4{\cdot}2CH_2Cl_2$: C, 39.06; H, 2.59. Found: 38.95; H, 2.81. IR frequencies (cm^{-1}) (CH_2Cl_2): ν(C≡O) 1986 w, 1964 vs, 1902 m, 1874 m.

Preparation of 8. A 8-mL volume of a xylene solution of **1** (0.08 g; 0.10 mmol) and diphenylethine (0.02 g; 0.11 mmol) was heated 6 h under reflux of the solvent. The colorless solution became yellow. Afterward, the solvent was removed and the product from the remaining solid was separated chromatographically (PSC plate, silica gel 60) with 5:1 *n*-hexane/$CDCl_3$ as eluant. From the yellow layer was obtained the orange compound **8** (0.02 g; 20.9%). Anal. Calcd for **8**: C, 40.95; H, 2.31. Found: C, 40.61; H, 2.52. IR frequencies (cm^{-1}) ($CDCl_3$): ν(C≡O) 2073 m, 2020 s, 1980 s, 1965 s, 1943 m, 1913 m. ^1H NMR data (δ) ($CDCl_3$): 7.40 (m, 20 H), 5.11 (d, vinylic H); ^1J(PH) = 8.8 Hz. ^{31}P NMR data (δ): 60.74 (s, μ-PPh_2).

Cyclic Voltammetric Measurements. These were undertaken with the following equipment: measuring cell (Fa. Methrom E 505), potentiostat (Fa. Wenking HP 72) and scan generator (VSG 72), and XY plotter (Fa. Philips PM 8132). The system of three electrodes used consisted of a planar platinum or gold electrode as the working electrode, a platinum wire, and a Ag/AgCl electrode in a saturated ethanolic solution of lithium chloride as the reference electrode. The samples were measured in dichloromethane solution in the presence of tetrabutylammonium hexafluorophosphate ((TBA)PF_6). The measured redox potentials $E^f = (E_{p,a} + E_{p,c})/2$ were related to $E^f(Fc^+/Fc)$ of ferrocene (Fc^+/Fc = 400 mV vs NHE) used as an internal standard. The evaluation of the cyclic voltammograms was done according to criteria of Nicholson and Shain (*Anal. Chem.* **1964**, *36*, 706).

X-ray Analysis of $[C_8H_{20}N][2]$. Lattice parameters were refined from 30 reflections with $11 \le 2\theta \le 30°$. Reflections were collected on a Nicolet R 3m/V diffractometer, ω–2θ scan, with Lp and absorption corrections (ψ scans) applied. The structure was solved by direct and Fourier methods. Full-matrix least-squares refinement was based on *F*. Re, P, O, N, and the carbonyl groups were refined anisotropically. Phenyl groups were treated as rigid bodies (C–C = 1.395 Å, C–H = 0.96 Å). H atom positions were fixed from geometrical considerations with isotropic displacement parameters U_{iso} = 0.09 Å^2. Further information is given in Table II.

X-ray Analysis of 3. The crystal measured at 293 K was sealed in a capillary. Lattice parameters were refined from 20 reflections with $8 \le 2\theta \le 25°$. The space group was determined from Buerger precession photographs. Reflections were collected on a R 3m/v diffractometer. The measurement of the reflections showed a decrease of 5% in intensities, scaled on standards. LP and empirical absorption correction via ψ scans were applied. The structure was solved by direct and Fourier methods. Full-matrix least-squares refinement was based on *F*. All atoms but the phenyl carbons were refined anisotropically; phenyl groups and H atoms were treated as above. Remaining features are depicted in Table II.

X-ray Analysis of 4. The lattice parameters were refined from 31 reflections with $7 \le 2\theta \le 27°$. The space group was determined from Weissenberg photographs. Reflections were collected on a R 3m/V diffractometer, ω–2θ scan, with Lp and absorption corrections (ψ scans) applied. Structure solving and refinement were as described for **3**. Au,

(4) (a) Braunstein, P.; Rose, J. *Gold Bull.* **1985**, 17. (b) Boyle, P. D.; Boyd, D. C.; Mueting, A. M.; Pignolet, L. H. *Inorg. Chem.* **1988**, *27*, 4424. (c) Moehring, G. A.; Fanwick, P. E.; Walton, R. A. *Inorg. Chem.* **1987**, *26*, 1861.
(5) (a) Hall, K. P.; Mingos, D. M. P. *Prog. Inorg. Chem.* **1984**, *32*, 237. (b) Owen, S. M. *Polyhedron* **1988**, *7*, 253 and references therein.

Table II. Crystal Data for $[C_8H_{20}N][2]$, **3**, **4**, **7**, and **8**[a]

	$[C_8H_{20}N][2]$	**3**	**4**	**7**	**8**
formula	$[C_{20}H_{10}O_8P\text{-}Re_2][C_8H_{20}N]$	$AuC_{38}H_{25}O_8P_2Re_2\cdot CH_2Cl_2$	$Au_2C_{61}H_{45}O_7P_3Re_2$	$Au_3C_{72}H_{55}O_6P_4Re_2\cdot 2CH_2Cl_2$	$C_{33}H_{21}O_7PRe_2$
mol wt	911.9	1325.8	1749.3	2273.3	932.9
space group (No.)	$C2/c$ (15)	$P\bar{1}$ (2)	$P2_1/n$ (14)	$P\bar{1}$ (2)	$P\bar{1}$(2)
a, Å	18.007 (3)	14.918 (7)	24.434 (4)	13.676 (5)	9.436 (2)
b, Å	17.165 (3)	15.456 (4)	10.284 (2)	13.817 (4)	11.774 (3)
c, Å	21.368 (5)	9.229 (4)	24.618 (4)	21.723 (7)	14.353 (4)
α, β, γ, deg	β = 109.36 (1)	93.12 (1), 97.10 (1), 83.27 (1)	β = 113.75 (1)	71.26 (1), 87.05 (1), 82.37 (1)	95.91 (2), 99.57 (2), 95.71 (2)
V, Å^3	6231.2	2095.4	5662.1	3852.6	1552.6
Z	8	2	4	2	2
D_{calcd}, g cm^{-3}	1.944	2.101	2.052	1.959	1.995
μ, cm^{-1}	79.70	95.80	96.12	91.25	74.41
transm coeff	0.054/0.102	0.260/0.411	0.453/0.77	0.104/0.462	0.026/0.065
R, R_w[b]	0.0446, 0.0355	0.0663, 0.0549	0.0718, 0.0561	0.0772, 0.0715	0.0516, 0.0556

[a] For all the structures, Mo Kα radiation was used and T = 296 K. [b] $w = 1/\sigma^2(F) + 0.0001F^2$.

Table III. $[C_{20}H_{10}O_8PRe_2][C_8H_{20}N]$ ($[C_8H_{20}N][2]$): Atomic Coordinates (×10^4) and Equivalent Isotropic Displacement Parameters (Å^2 × 10^3)

	x	y	z	U(eq)
Re(1)	1742 (1)	9584 (1)	1914 (1)	40 (1)
Re(2)	3102 (1)	10754 (1)	2266 (1)	44 (1)
P(1)	1871 (2)	10808 (2)	2492 (1)	38 (2)
C(1)	1240 (7)	10131 (7)	1053 (6)	64 (9)
C(2)	2196 (7)	9058 (7)	2787 (6)	54 (8)
C(3)	2180 (8)	8786 (8)	1476 (6)	63 (10)
C(4)	734 (8)	9159 (6)	1831 (6)	49 (8)
C(5)	3803 (9)	10243 (9)	1878 (8)	108 (14)
C(6)	2553 (7)	11328 (8)	1416 (7)	60 (9)
C(7)	3685 (8)	11657 (9)	2614 (6)	70 (10)
C(8)	3591 (7)	10198 (7)	3134 (7)	52 (9)

Scheme I

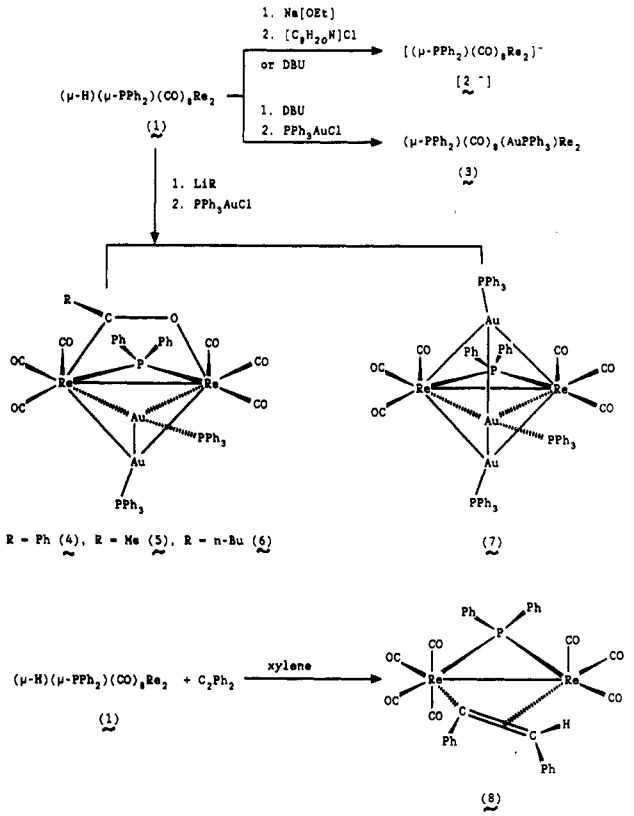

Re, and P were refined anisotropically.

X-ray Analysis of 7. The crystal measured at 293 K was sealed in a capillary. The lattice parameters were refined from 30 reflections with $10 \le 2\theta \le 30°$. The space group was determined from Buerger precession photographs. Reflections were collected on a Nicolet R 3m/V diffractometer, ω–2θ scan (scan speed 7.2°/min), and Lp and absorption corrections (ψ scans) applied. The rapid scan was necessary because of loss of coordinated dichloromethane. There was a decrease of 15% in intensities, scaled on standards. Structure solving and refinement were as described for **3**. Au, Re, P, and Cl were refined anisotropically.

X-ray Analysis of 8. The lattice parameters were refined from 20 reflections with $4 \le 2\theta \le 24°$. Data collection, corrections, and structure solving and refinement were as described for **3**. Re and P were refined anisotropically.

Table IV. $AuC_{38}H_{25}O_8P_2Re_2\cdot CH_2Cl_2$ (**3**): Atomic Coordinates (×10^4) and Equivalent Isotropic Displacement Parameters (Å^2 × 10^3)

	x	y	z	U(eq)
Au(1)	686 (1)	2441 (1)	−731 (2)	41 (1)
Re(1)	2007 (1)	2322 (1)	−2677 (2)	36 (1)
Re(2)	2288 (1)	2939 (1)	728 (2)	36 (1)
P(1)	3278 (5)	2870 (6)	−1156 (10)	38 (5)
P(2)	−859 (6)	2287 (6)	−868 (9)	41 (5)
C(1)	3192 (25)	3400 (22)	2234 (35)	45 (23)
C(2)	1373 (24)	2852 (28)	2125 (42)	65 (28)
C(3)	1663 (25)	4155 (26)	173 (35)	53 (25)
C(4)	2809 (23)	1693 (23)	1168 (39)	51 (23)
C(5)	1629 (23)	3550 (27)	−3284 (39)	56 (26)
C(6)	2615 (20)	2035 (24)	−4340 (36)	44 (23)
C(7)	805 (24)	1984 (22)	−3741 (37)	48 (23)
C(8)	2239 (26)	1020 (28)	−2046 (38)	55 (26)

Table V. $Au_2C_{61}H_{45}O_7P_3Re_2$ (**4**): Atomic Coordinates (×10^4) and Equivalent Isotropic Displacement Parameters (Å^2 × 10^3)

	x	y	z	U(eq)
Au(1)	9258 (1)	2386 (1)	2378 (1)	50 (1)
Au(2)	10008 (1)	1933 (2)	1821 (1)	55 (1)
Re(1)	8809 (1)	2991 (1)	1149 (1)	42 (1)
Re(2)	9049 (1)	112 (1)	1583 (1)	45 (1)
P(1)	9520 (4)	2745 (10)	3369 (4)	60 (6)
P(2)	10986 (4)	2488 (10)	2025 (4)	61 (6)
P(3)	8102 (4)	1273 (9)	1124 (4)	50 (6)
C(7)	9021 (12)	1660 (29)	576 (13)	38 (8)
O(7)	9055 (9)	490 (21)	709 (9)	55 (6)

Table VI. $Au_3C_{72}H_{55}O_6P_4Re_2\cdot 2CH_2Cl_2$ (**7**): Atomic Coordinates (×10^4) and Equivalent Isotropic Displacement Parameters (Å^2 × 10^3)

	x	y	z	U(eq)
Au(1)	3901 (1)	5696 (1)	2167 (1)	42 (1)
Au(2)	2544 (1)	4317 (1)	2192 (1)	40 (1)
Au(3)	2751 (1)	2648 (1)	3371 (1)	40 (1)
Re(1)	3004 (1)	4654 (1)	3360 (1)	35 (1)
Re(2)	4424 (1)	3539 (1)	2706 (1)	35 (1)
P(1)	3850 (9)	7412 (8)	1522 (5)	46 (7)
P(2)	1588 (9)	4523 (8)	1318 (5)	44 (7)
P(3)	1605 (9)	1563 (8)	3939 (5)	42 (7)
P(4)	4706 (8)	4031 (8)	3651 (5)	37 (6)

Results

The transformations observed in this work are summarized in Scheme I. A structure study was undertaken for the complexes **2**$^-$–**4**, **7**, and **8**, whose crystal data, positional parameters of selected atoms, and selected bond angles and bond lengths are presented in Tables II–IX. View of their molecular structures are shown

Table VII. $C_{33}H_{21}O_7PRe_2$ (**8**): Atomic Coordinates ($\times 10^4$) and Equivalent Isotropic Displacement Parameters ($Å^2 \times 10^3$)

	x	y	z	U(eq)
Re(1)	643 (1)	3875 (1)	2763 (1)	43 (1)
Re(2)	3777 (1)	3509 (1)	3050 (1)	45 (1)
P(1)	2390 (3)	4479 (3)	1794 (2)	43 (2)
C(1)	-1178 (15)	3762 (11)	1945 (10)	52 (8)
C(2)	511 (14)	5490 (13)	3190 (10)	55 (9)
C(3)	-417 (16)	3462 (13)	3765 (11)	66 (10)
C(4)	3354 (13)	4543 (12)	4099 (11)	49 (8)
C(5)	4242 (13)	2374 (12)	2045 (11)	51 (8)
C(6)	4743 (15)	2626 (13)	3985 (10)	58 (9)
C(7)	5516 (15)	4514 (12)	3009 (10)	54 (8)
C(8)	1736 (15)	2249 (10)	2903 (9)	51 (8)
C(9)	865 (13)	2015 (9)	2004 (9)	42 (7)

Table VIII. Selected Bond Lengths (Å) and Bond Angles (deg)

$[C_{20}H_{10}O_8PRe_2][C_8H_{20}N]$ ($[C_8H_{20}N][\mathbf{2}]$)

Re(1)-Re(2)	3.062 (1)	Re(1)-P(1)	2.409 (3)
Re(1)-C(1)	1.996 (13)	Re(1)-C(2)	1.987 (12)
Re(1)-C(3)	1.966 (13)	Re(1)-C(4)	1.909 (10)
Re(2)-P(1)	2.422 (2)	Re(2)-C(5)	1.935 (13)
Re(2)-C(6)	2.013 (13)	Re(2)-C(7)	1.882 (14)
Re(2)-C(8)	2.012 (13)		

Re(2)-Re(1)-P(1)	50.9 (1)	Re(2)-Re(1)-C(1)	89.9 (3)
Re(2)-Re(1)-C(2)	91.2 (3)	Re(2)-Re(1)-C(3)	99.2 (3)
Re(2)-Re(1)-C(4)	158.7 (3)	Re(1)-Re(2)-P(1)	50.5 (1)
Re(1)-Re(2)-C(5)	100.4 (4)	Re(1)-Re(2)-C(6)	89.2 (3)
Re(1)-Re(2)-C(7)	159.0 (3)	Re(1)-Re(2)-C(8)	89.1 (3)
Re(1)-P(1)-Re(2)	78.6 (1)	P(1)-Re(1)-C(1)	90.0 (4)
P(1)-Re(1)-C(2)	88.6 (4)	P(1)-Re(1)-C(3)	150.1 (3)
P(1)-Re(1)-C(4)	107.9 (3)	P(1)-Re(2)-C(5)	150.8 (4)
P(1)-Re(2)-C(6)	87.3 (3)	P(1)-Re(2)-C(7)	108.5 (4)
P(1)-Re(2)-C(8)	89.1 (2)		

$AuC_{38}H_{25}O_8P_2Re_2 \cdot CH_2Cl_2$ (**3**)

Au(1)-Re(1)	2.810 (2)	Au(1)-Re(2)	2.764 (2)
Au(1)-P(2)	2.332 (8)	Re(1)-Re(2)	3.225 (2)
Re(1)-P(1)	2.422 (8)	Re(2)-P(1)	2.408 (9)

Re(1)-Au(1)-Re(2)	70.7 (1)	Au(1)-Re(1)-Re(2)	54.0 (1)
Re(2)-Re(1)-C(5)	91.8 (10)	Re(2)-Re(1)-C(6)	143.8 (10)
Re(2)-Re(1)-C(7)	123.9 (10)	Re(2)-Re(1)-C(8)	88.8 (10)
Au(1)-Re(2)-Re(1)	55.3 (1)	Re(1)-Re(2)-C(1)	141.7 (10)
Re(1)-Re(2)-C(2)	123.9 (11)	Re(1)-Re(2)-C(3)	88.9 (9)
Re(1)-Re(2)-C(4)	87.7 (10)	Re(1)-P(1)-Re(2)	83.8 (3)

$Au_2C_{61}H_{45}O_7P_3Re_2$ (**4**)

Au(1)-Au(2)	2.734 (1)	Au(1)-Re(1)	2.841 (2)
Au(1)-Re(2)	2.960 (2)	Au(1)-P(1)	2.291 (9)
Au(2)-Re(1)	2.933 (2)	Au(2)-Re(2)	2.869 (2)
Au(2)-P(2)	2.306 (6)	Re(1)-Re(2)	3.122 (2)
Re(1)-P(3)	2.454 (7)	Re(1)-C(7)	2.172 (26)
Re(2)-P(3)	2.440 (7)	Re(2)-O(7)	2.191 (19)
C(7)-O(7)	1.241 (36)		

Au(2)-Au(1)-Re(1)	63.5 (1)	Au(2)-Au(1)-Re(2)	60.3 (1)
Re(1)-Au(1)-Re(2)	65.1 (1)	Au(1)-Au(2)-Re(1)	60.0 (1)
Au(1)-Au(2)-Re(2)	63.7 (1)	Re(1)-Au(2)-Re(2)	65.1 (1)
Au(1)-Re(1)-Au(2)	56.5 (1)	Au(1)-Re(1)-Re(2)	59.3 (1)
Au(1)-Re(1)-C(7)	117.6 (8)	Au(2)-Re(1)-Re(2)	56.5 (1)
Au(2)-Re(1)-C(7)	71.8 (6)	Re(2)-Re(1)-C(7)	64.1 (8)
Au(1)-Re(2)-Au(2)	55.9 (1)	Au(1)-Re(2)-Re(1)	55.6 (1)
Au(1)-Re(2)-O(7)	116.2 (6)	Au(2)-Re(2)-Re(1)	58.5 (1)
Au(2)-Re(2)-O(7)	76.0 (5)	Re(1)-Re(2)-O(7)	64.6 (6)
Re(1)-P(3)-Re(2)	79.3 (2)	Re(1)-C(7)-O(7)	116.7 (18)
Re(2)-O(7)-C(7)	113.8 (17)		

in Figures 1-5. Finally, ^{31}P NMR spectroscopic, electrochemical, and reactivity studies were undertaken and are presented in Tables I, X, and XI.

Discussion

Deprotonation of 1 and Reaction with Ph_3AuCl To Give 3. Covalent and saltlike organometallic substances with a Re-Au bond have been published, for example $PPh_3AuRe(CO)_5$,[6] [(μ-Cp)(CO)(*p*-$N_2C_6H_4OMe$)ReAuPPh_3^+],[7] $[Ph_4As]_2$-$[PPh_3AuRe_7C(CO)_{27}]$,[8] $[PPh_3AuRe_3(\mu\text{-}H)_3(CO)_{10-n}]^-$ (n = 0, 1),[9] and $[PPh_3AuRe_2(\mu\text{-}Br)(CO)_6((EtO)_2POP(OEt_2)_2)]$.[10] To obtain further compounds with this Au-Re bond, our first efforts were directed on the deprotonation of **1** with the strong base NaOEt in ethanolic solution. The reactants give in boiling ethanol solution the yellow anion $[Re_2(CO)_8(\mu\text{-}PPh_2)]^-$ ($\mathbf{2}^-$) (Scheme II), which has been precipitated as tetraethylammonium salt $[C_8H_{20}N][\mathbf{2}]$ (yield 24%). Because of a very low solubility of **1** in ethanol, the better solvent THF and the base DBU were used to deprotonate **1**. At room temperature **1** was converted into $\mathbf{2}^-$, which was then reacted with PPh_3AuCl (see Scheme II, step ii) to give the yellow substance $[(\mu\text{-}PPh_2)(CO)_8Re_2AuPPh_3]$ (**3**) (yield 52%). This sequence provides for the isolobal exchange of H vs $AuPPh_3$ as expected.[3] Both types of products $[C_8H_{20}N][\mathbf{2}]$ and **3** have been identified through single-crystal X-ray analyses. The δ values of their $^{31}P\{H\}$ NMR spectra are given in Table I.

Deprotonations Accompanied by Acylation Leading to Products 4-6. Our further efforts with the nucleophiles LiR (R = Me, *n*-Bu, Ph) for cluster formation were started for each LiR and **1** in THF solution with a 2:1 molar ratio at -78 °C. After each reaction solution reached room temperature (Scheme II, steps i and iii, with intermediates $\mathbf{A}^{2-}$ and $\mathbf{B}^{2-}$), an amount of PPh_3AuCl was added that was equimolar to the amount previously added LiR. The TLC separation procedure of these solutions gave two types of products: first, acyl-bridged derivatives $[(\mu\text{-}C(R)O)(\mu\text{-}PPh_2)(CO)_6Re_2Au(PPh_3)_2]$ (R = Ph (**4**), yield of 31%; R = Me (**5**), 27%; R = *n*-Bu (**6**), 21%) and second, $[(\mu\text{-}PPh_2)$-

Table IX. Selected Bond Lengths (Å) and Bond Angles (deg)

$Au_3C_{72}H_{55}O_6P_4Re_2 \cdot 2CH_2Cl_2$ (**7**)

Au(1)-Au(2)	2.818 (3)	Au(1)-Re(1)	2.836 (2)
Au(1)-Re(2)	2.836 (3)	Au(2)-Au(3)	2.840 (3)
Au(2)-Re(1)	2.838 (3)	Au(2)-Re(2)	2.793 (3)
Au(3)-Re(1)	2.832 (3)	Au(3)-Re(2)	2.846 (3)
Re(1)-Re(2)	2.914 (3)	Re(1)-P(4)	2.414 (13)
Re(2)-P(4)	2.423 (12)		

Au(2)-Au(1)-Re(1)	60.3 (1)	Au(2)-Au(1)-Re(2)	59.2 (1)
Re(1)-Au(1)-Re(2)	61.8 (1)	Au(1)-Au(2)-Au(3)	109.4 (1)
Au(1)-Au(2)-Re(1)	60.2 (1)	Au(1)-Au(2)-Re(2)	60.7 (1)
Au(3)-Au(2)-Re(1)	59.8 (1)	Au(3)-Au(2)-Re(2)	60.7 (1)
Re(1)-Au(2)-Re(2)	62.3 (1)	Au(2)-Au(3)-Re(1)	60.0 (1)
Au(2)-Au(3)-Re(2)	58.8 (1)	Re(1)-Au(3)-Re(2)	61.8 (1)
Au(1)-Re(1)-Au(2)	59.5 (1)	Au(1)-Re(1)-Au(3)	109.1 (1)
Au(1)-Re(1)-Re(2)	59.1 (1)	Au(2)-Re(1)-Au(3)	60.1 (1)
Au(2)-Re(1)-Re(2)	58.1 (1)	Au(3)-Re(1)-Re(2)	59.3 (1)
Au(1)-Re(2)-Au(2)	60.1 (1)	Au(1)-Re(2)-Au(3)	108.7 (1)
Au(1)-Re(2)-Re(1)	59.1 (1)	Au(2)-Re(2)-Au(3)	60.5 (1)
Au(2)-Re(2)-Re(1)	59.6 (1)	Au(3)-Re(2)-Re(1)	58.9 (1)
Re(1)-P(4)-Re(2)	74.1 (3)		

$C_{33}H_{21}O_7PRe_2$ (**8**)

Re(1)-Re(2)	2.998 (1)	Re(1)-P(1)	2.427 (3)
Re(1)-C(1)	1.896 (12)	Re(1)-C(2)	1.960 (14)
Re(1)-C(3)	1.957 (14)	Re(1)-C(8)	2.274 (10)
Re(1)-C(9)	2.387 (10)	Re(2)-P(1)	2.490 (3)
Re(2)-C(4)	1.957 (14)	Re(2)-C(5)	1.997 (14)
Re(2)-C(6)	1.945 (13)	Re(2)-C(7)	1.938 (11)
Re(2)-C(8)	2.277 (10)	C(8)-C(9)	1.394 (17)

Re(2)-Re(1)-P(1)	53.4 (1)	Re(2)-Re(1)-C(8)	48.8 (3)
Re(2)-Re(1)-C(9)	71.0 (2)	P(1)-Re(1)-C(8)	87.9 (3)
P(1)-Re(1)-C(9)	82.5 (3)	Re(1)-Re(2)-P(1)	51.5 (1)
Re(1)-Re(2)-C(8)	48.8 (3)	P(1)-Re(2)-C(8)	86.4 (3)
Re(1)-P(1)-Re(2)	75.1 (1)	C(21)-P(1)-C(31)	102.9 (4)
Re(1)-C(8)-Re(2)	82.4 (4)	Re(1)-C(8)-C(9)	77.1 (6)
Re(2)-C(8)-C(9)	117.1 (8)	Re(1)-C(9)-C(8)	68.2 (6)

(6) Bower, L.; Stiddard, M. H. *J. Chem. Soc. A* **1968**, 706.
(7) Barrientos-Penna, C. F.; Einstein, F. W. B.; Jones, T.; Sutton, D. *Inorg. Chem.* **1985**, *24*, 632.
(8) Henly, T. J.; Shapley, J. R.; Rheingold, A. L. *J. Organomet. Chem.* **1986**, *310*, 55.
(9) Beringhelli, T.; Ciani, G.; D'Alfonso, G.; De Malde, V.; Freni, M. *J. Chem. Soc., Chem. Commun.* **1986**, 735.
(10) Riera, V.; Ruiz, A. M.; Tripicchio, A. *J. Chem. Soc., Dalton Trans.* **1987**, 1551.

Scheme II

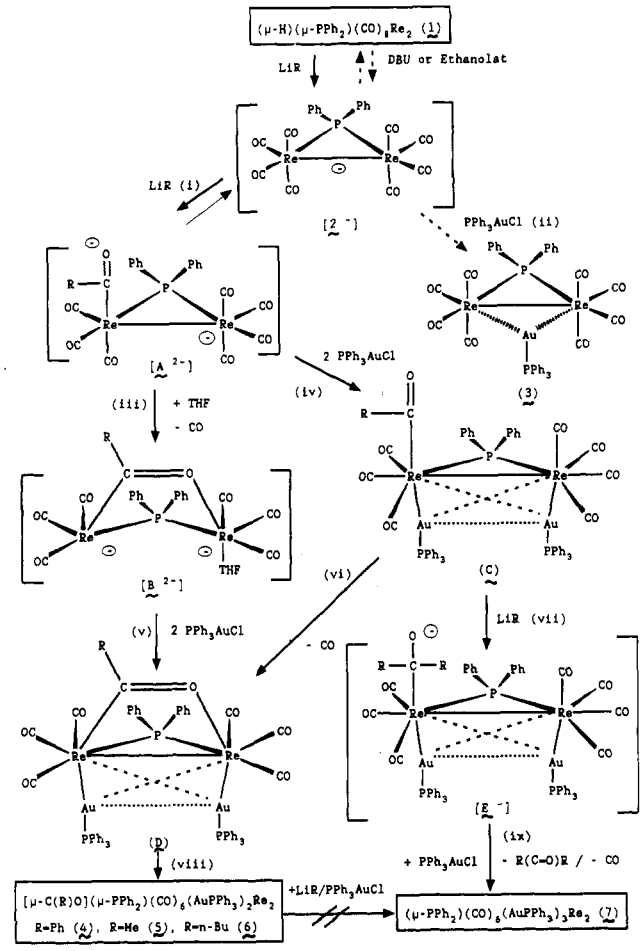

$(CO)_6Re_2(AuPPh_3)_3]$ (7) (R = Ph, 2%; R = Me, 4%; R = *n*-Bu, 1%). Both types of products have been identified through the related results of single-crystal X-ray analyses. The other two acyl-bridged derivatives **5** and **6** were characterized by comparison of their spectroscopic data, including their $^{31}P\{H\}$ NMR data (Table I).

As mentioned in the introductory remarks, with the nucleophiles used a reaction pattern with release of RH and acylation is expected, since Kaesz et al.[11] have also reported low-temperature nucleophilic alkylation of a polynuclear hydride complex, followed by elimination of aldehyde. Besides that, we were not able to find reaction conditions for a selective deprotonation of **1** by LiMe in the temperatue range between −78 and 0 °C. Instead, we observed the proposed intermediates A^{2-} and B^{2-} (Scheme II, steps i and iii), which are supported by accompanied ^{31}P and ^{13}C NMR measurements (see later). This result is in accordance with an absence of **3** in the product mixture.

From present knowledge of the reactivity of phosphido-bridged bimetallic complexes with a metal–metal bond, the pair of CO ligands positioned trans to the μ-P in $\mathbf{2}^-$ are subjected to both nucleophilic attack at the C atom and ligand dissociation.[1,12,13] Therefore, the subsequent entry of two $AuPPh_3$ fragments might be possible in cis positions, which facilitate a redox condensation process between the gold atoms under formation of an Au_2Re_2 core of the metallahedrane type. The related Au_2Re_2 core and that of Au_3Re_2 in **7** have as a common feature three carbonyl ligands of idealized C_{3v} symmetry at each Re atom. This carbonyl entity stabilizes the molecules from further substitution and auration.

Proposed Pathway for the Formation of 5 and 7. The preparative results with respect to the substances **4**–**7** encompass several reaction steps, which are presented in Scheme II. As a general description for the complex reaction course, it can be said that at first the pathway i comprising the deprotonation of the μ-H atom in **1** under release of RH and the simultaneous nucleophilic attack on one carbonylic C atom to form a terminally bonded acylic ligand resulting in the intermediate A^{2-} takes place. Second, the subsequent reactions of A^{2-} are determined by the competitive routes iii and iv, of which route iii mediates the formation of the main product with an Re_2Au_2 core, **5**, while route iv leads to a further common intermediate C, which opens a route to the by-product with an Re_2Au_3 core, **7**, and the main product, **5**. Scheme II shows that these product formations are accompanied by an uptake of $[PPh_3Au^+]$ cations, routes iv, v, and ix, a CO substitution reaction originated from the formation of an acylic bridging group, routes iii and iv, a conversion of a C(R)O group by R^- into a ketone leaving group, route ix, and finally redox condensation processes, routes viii and ix. Supporting facts for some of the given reaction steps in Scheme II were obtained by separate experiments. At first it was ascertained that **5** cannot be converted with LiMe and PPh_3AuCl under loss of MeCOMe into **7**, since **5** underwent no reaction with LiMe in boiling THF solution over a 10-h period. We thus ruled out that **5** is a precursor to **7**. Other experiments were undertaken to get knowledge of the reaction pathway leading to **5** and **7**. The reactants **1** and LiMe were placed in THF-d_8 solution, and the solutions were held at −78 °C for 1 h and than warmed to room temperature for ^{31}P NMR measurements. Two singlets with δ values of 25.8 and of −116.4 were observed. Two singlets are also observed in the ^{13}C NMR spectra with δ 54.0 and 56.0. From the absence of a $J(PP)$ coupling constant in the ^{31}P NMR spectrum, it can be concluded that two solvent species had been formed. Regarding literature data, both $\delta(^{13}C)$ values are typical for a Me groups in acyl fragments, for example, in the compounds $Na[Fe_2(\mu\text{-}PPh_2)(CO)_5(C(Me)O)]\cdot 2THF$ and $Na[Fe(CO)_4(C(Me)O)]$.[14,15] On the basis of these results, it is not unreasonable to postulate the subsequent solvent species $[Re_2(CO)_7(C(Me)O)(\mu\text{-}PPh_2)]^{2-}$ (A^{2-}) and $[Re_2(CO)_6(thf)(\mu\text{-}C(Me)O)(\mu\text{-}PPh_2)]^{2-}$ (B^{2-}) (Scheme II). The proposal takes into account the present knowledge of $\delta(^{31}P)$ data, which demand for a μ-P atom in the absence of a metal–metal bond a low-field δ peak.[1,15] Consequently, the last-named solvent species can be assigned to δ −116.4 and the remaining one to δ 25.8. The conversion of **1** to **5** or **7** is proposed to occur through common anion $[Re_2(CO)_7(C(Me)O)(\mu\text{-}PPh_2)]^{2-}$ (A^{2-}). Suppression of CO loss in this species leads to **7**. To support this idea, a THF solution of **1** saturated with CO(g) in a suitable Schlenk tube was cooled to −50 °C, 2 equiv of LiMe was added, and afterward the solution was warmed to 20 °C for an addition of 2 equiv of PPh_3AuCl in the presence of a CO atmosphere. Through this procedure only **7** is formed. A second intermediate, the Re_2Au_2 species, C, may control the paths to **5** or **7**. Regrettably, a variation of the molar ratio of the three reactants does not allow further insight into their reaction course because of the occurrence of three simultaneous reaction paths with LiMe: deprotonation, (step i) nucleophilic attack at carbon of a CO group, or the transmetalation reaction to methylgold(I) compounds. The last case is favored when PPh_3AuCl is present in excess. This transmetalation reaction and additional unidentified substances are responsible for the fact that the yield of both cluster types remains somewhat below 50%. Of the lithium organyls used, LiMe gives double the yield of **7** as compared to LiPh. A reasonable explanation following Scheme II is the release of a ketone in step ix, which should be enhanced by the stronger nucleophile LiMe in step vii. This interpretation also correlates with the fact that the reagent lithium diisopropylamide (LDA), which is sterically hindered toward nucleophilic attack, generates no **7**.[17]

(11) Jensen, C. M.; Kaesz, H. D. *J. Organomet. Chem.* **1985**, *330*, 133.
(12) Breen, M. J.; Shulman, P. M.; Geoffroy, G. L.; Rheingold, A. L.; Fultz, W. C. *Organometallics* **1984**, *3*, 782; **1985**, *4*, 1418.
(13) Powell, J.; Contoure, C.; Gregg, M. R. *J. Chem. Soc., Chem. Commun.* **1988**, 1208.
(14) Winter, S. R. Ph.D. Thesis, Stanford University, Stanford, CA, 1973.
(15) Collemann, J. P.; Rothrode, R. K.; Finke, R. G.; Moore, E. J. *Inorg. Chem.* **1982**, *21*, 146.
(16) Garron, P. E. *Chem. Rev.* **1985**, *85*, 171.

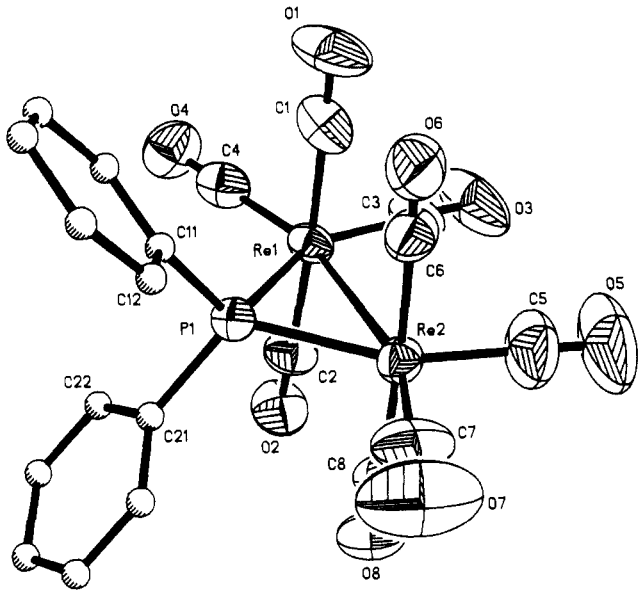

Figure 1. Molecular structure of 2^-, showing the atom-numbering scheme (50% tep (tep = thermal ellipsoid probability)).

Reaction with Acetylene. We were also successful in the hydrogen transfer in **1** to diphenylacetylene in boiling xylene. The unique product is the compound $Re_2(\mu\text{-}\sigma\text{:}\eta^2\text{-}CPh{=}CH(Ph))(\mu\text{-}PPh_2)(CO)_7$ (**8**). The substance was characterized by X-ray structure determination. The migration of the hydrido bridging ligand is thermally initiated. By contrast to that, the photochemical reaction between $Re_3(\mu\text{-}H)_3(CO)_{12}$ and tolan gives $Re_2H_2(CO)_7(CPh{=}CPh)$ and comparable π-complexes without a hydrido ligand.[18]

Structural Descriptions. Anion 2^-. The molecular structure of the anion $[(\mu\text{-}PPh_2)(CO)_8Re_2]^-$ (Figure 1) has a triangular $Re_2(\mu\text{-}P)$ atom arrangement of idealized C_{2v} symmetry. At the independent Re atoms four corresponding pairs of the terminal CO ligands are arranged in eclipsed positions. Such a conformation indicates an absence of repulsive nonbonding forces between the CO ligands. The structurally known substance $[Re_2(\mu\text{-}H)(\mu\text{-}PPh_2)(CO)_7PPh_3]$ has the same $Re_2(\mu\text{-}P)$ fragment with three eclipsed pairs of terminal CO ligands at the Re atoms.[1] The effect of the deprotonation becomes visible by going from the last-named substance to 2^-; the (μ-P)–Re bond length is shortened from 2.430 (4) to 2.416 (3) Å, and the Re–Re bond length from 3.152 (1) to 3.062 (1) Å, including the simultaneous reduction of the Re–(μ-P)–Re ring angle of 3.0 (1)°. The shortening of the metal–metal bond by deprotonation is consistent with the lengthening of hydrido-bridged metal–metal bonds.[19,20]

The most striking difference between the structures of 2^- and those considered is the orientation of the carbonyl ligands around the metal centers, which can be correlated with the absence of the μ-H ligand in 2^-. For example, the carbonyl ligands trans to the phosphido bridge move to fill the vacant coordination site created by removal of the hydride ligand. The Re–Re–C angle in the hydride compound is 123.5 (3)° while in 2^- it is 99.8 (5)°. This migration is accompanied by enlargement of the (μ-P)–Re–C angle in 2^- by 8.3 (8)°. The Re–CO bond lengths in 2^- vary according to the nature of the trans or pseudotrans ligands. Thus, the average Re–C CO trans to CO distance, 2.002 (13) Å, is longer than both the Re–C (CO pseudotrans to PPh_2), average 1.951 (15) Å, and Re–C (axial CO) distance, average 1.896 (14) Å. This last length shows the expected shortening on replacement of a pseudotrans phosphine by a metal–metal bond.

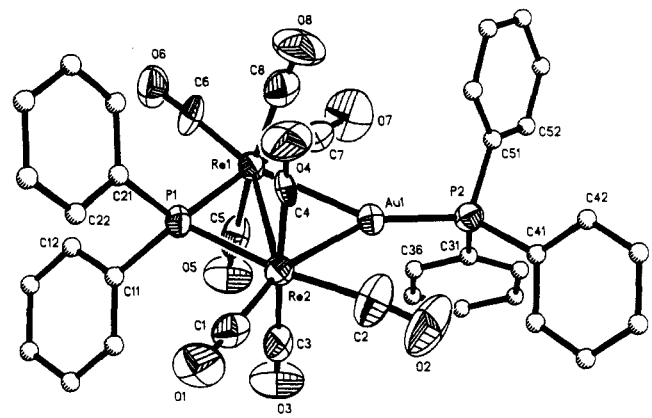

Figure 2. Molecular structure of **3**, showing the atom-numbering scheme (50% tep).

Complex 3. The diamagnetic compound **3** (Figure 2) crystallizes as solvate with one molecule of dichloromethane. The independent Re atoms show octahedrally distorted coordination closely analogous to that in the isolobal compounds $Re_2(\mu\text{-}H)(\mu\text{-}PPh_2)(CO)_{8-n}(PPh_3)_n$ (n = 1, 2).[1] When viewed along their Re–Re bond, the trans-positioned carbonyl ligands in **3** are approximately staggered, whereas those of the hydride complex (n = 1) are approximately eclipsed. To illustrate this geometrical situation, the dihedral angles between the Re(μ-P)Re plane and each $Re_2C(Y)$ plane are given for each C(Y): C(1), 0.1°; C(2), 4.6°; C(6), 11.9°; C(7), 5.7°. The conformational difference between **3** and the hydride derivative (n = 1) may be due to the increased steric bulk of the gold phosphine as compared to the bridged hydrido ligand. The larger steric requirement is also seen in the movement of cis carbonyl groups away from the bridging gold atom. Thus, the Re–Re–C (CO trans to PPh_2) angle increases from 116.9 (6)° in the hydride (n = 1) to 123.9 (11)° in **3**. In the anion 2^- this angle decreases to 99.8° due to the carbonyl moving to fill the vacant site. Such a site is occupied in **3**, and its $AuPPh_3$ is part of the central molecular fragment $Re_2(\mu\text{-}P)Au$ in which the gold atom lies 0.18 Å above the $Re_2(\mu\text{-}P)$ plane.

The Re–Re bond length of 3.225 (2) Å in **3** is longer than those of 3.152 (1) Å in the hydride derivative (n = 1) and of 3.194 (1) Å in the corresponding substance (n = 2). Accompanying the increased bond length, an additional enlargement of the bond angle at the μ-P atom takes place from 81.6 (1)° in the hydride derivative (n = 1) to 83.8 (3)° in **3**. The elongation of the Re–Re bond in **3** may be due to the greater steric requirements of the $AuPPh_3$ group. Both related Re–Au bond lengths of 2.810 (2)° and of 2.764 (2) Å are significantly different. The molecular structure of **3** in the crystal shows that intramolecular nonbonding contact lengths between neighboring Ph residues of PPh_3 and the carbonyl groups along the Au(1)–Re(1) vector are distinctly shorter than those along the Au(1)–Re(2) vector. This is also supported by the deviation of the subtended Re–Au–P bond angles of 15.1 (2)°. The origin of geometrical deformations should result from packing forces, which are observed for similar compounds.[21] The average Au–Re bond length of 2.787 (2) Å is consistent with the values reported for other rhenium compounds with an Au–Re single bond, for example, 2.837 (1) Å in $[Ph_4P][Re_3(\mu\text{-}H)_3(CO)_9AuPPh_3]$[9] and 2.873 (1) Å in $[Ph_4As]_2[Re_7C(CO)_{21}AuPPh_3]$.[8]

Effect of Bridging $AuPPh_3$. A close structural analogy exists between the bridging hydride and bridging gold phosphine in the dirhenium compounds. The principal structural difference between the dirhenium complexes resulting from bridging the Re–Re bond in **3** with a gold phosphine as compared to a hydride are first, an increase in the Re–Re bond length, second, displacement of CO ligands away from the bridging ligand, and third, a small increase in the bond angle at the μ-P atoms. Such facts may be rationalized

(17) Haupt, H.-J.; Heinekamp, C.; Flörke, U. *Z. Anorg. Allg. Chem.*, in press.
(18) Epstein, R. A.; Gaffroy, T. R.; Geoffroy, G. L.; Gladfelter, W. L.; Henderson, R. S. *J. Am. Chem. Soc.* **1979**, *101*, 3847.
(19) Kaesz, H. D.; Saillant, R. B. *Chem. Rev.* **1972**, *72*, 231.
(20) Churchill, M. R.; De Boer, D. G.; Rotella, F. J. *Inorg. Chem.* **1976**, *15*, 1843.
(21) Haupt, H. J.; Preut, H. *Acta Crystallogr., Sect. C: Struct. Crystallogr. Cryst. Chem.* **1986**, *C42*, 275.

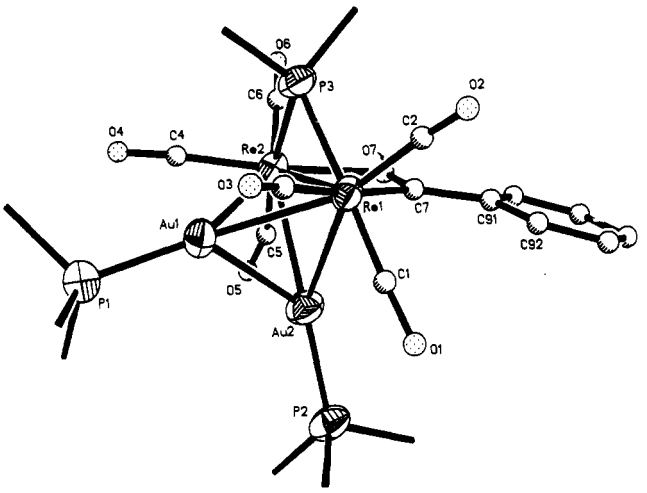

Figure 3. Molecular structure of **4**, showing the atom-numbering scheme (50% tep). Phenyl groups are omitted for the sake of clarity.

in terms of greater steric bulk of the gold phosphine group compared with that of a hydride ligand and additionally by electronic reasons that are responsible for lengthening metal–metal bonds in polynuclear hydrides.[19,20]

Complex 4. The tetrahedral Re_2Au_2 core in **4** (Figure 3) is of idealized C_{2v} symmetry. Each gold atom is coordinated with one PPh_3 ligand, whereas the dirhenium unit is bridged by a PPh_2 group. The coordination sphere at each Re atom is then completed with three terminal CO ligands that are nearly arranged in C_{3v} symmetry. The conformation of these CO ligands is approximately eclipsed. A valence electron count of 34 electrons is achieved in the diamagnetic substance **4** if each gold phosphine group is taken as a one-electron donor ligand as is usual.[5]

The presence of an Re–Re bond (Re–Re = 3.122 (2) Å) is in accordance with the acute bond angle subtended at the phosphorus atom of μ-PPh_2[1] and the observed geometrical shape of the μ-C(Ph)O group.[22] The latter bridge system has been described in terms of resonance between oxyalkylidene and acyl bonding modes, and evidently the two canonical forms contribute to the bonding in **4** also.[23] Thus, the C(7)–Re(1) bond length of 2.17 (3) Å is intermediate between the rhenium–alkylidene carbon distance of 1.92 (2) Å in $[Re(=CHSiPh_3)(CO)_2(\mu\text{-}C_6H_5)]$[24] and the rhenium–alkyl carbon distance of 2.302 (7) Å in $ReW(\mu\text{-}CH_2C_6H_4Me_4)(\mu\text{-}Me_2PCH_2PMe_2)(CO)_7]$.[25] Besides that, the C(7)–O(7) bond length of 1.24 (4) Å in **4** is similar to those previously observed for such distances in $MoIr(\mu\text{-}C(Me)O)(\mu\text{-}CO)(CO)(\eta\text{-}C_5H_5)_3$ (1.285 (3) Å),[23] $IrMn(\mu\text{-}C(Me)O)_2(\mu\text{-}PPh_2(CO)_3(\eta\text{-}C_5H_5)$ (1.26 (1) Å)[26] and $Fe_2(\mu\text{-}C(Ph)O)_2(CO)_6]$ (1.26 (1) Å).[27]

The inner Au_2Re_2 metallatetrahedron is distorted. This is shown by the average angles subtended at the following atoms: Au(1), 63.0 (1)°; Au(2), 62.9 (1)°; Re(1), 56.6 (1)°; Re(2), 56.6 (1)°. The values of related bond lengths are Au–Au = 2.734 (2) Å, Re–Re = 3.122 (2) Å, and Au–Re(av) = 2.901 (2) Å. These bond lengths are consistent with data previously reported for the various metal–metal single bonds, for example, listed as follows: Re–Re = 3.058 (1) Å in $Re_2[\mu\text{-}CHCHCMe_2](CO)_8$,[27] 3.104 (1) Å in $Re_2CO)_{10}$,[28] and 3.152 (1) Å in $Re_2(CO)_8(\mu\text{-}H)(\mu\text{-}PPh_2)$;[1] Au–Au = 2.800 (2) Å in $(PPhMe_2P)_3H_2Re(AuPPh_3)_3$;[29] Au–Re = 2.837 (1) Å in $[Re_3(\mu\text{-}H)_3(CO)_9(AuPPh_3)^-]$.[9] For a MO description of such mixed rhenium gold clusters, see ref 5.

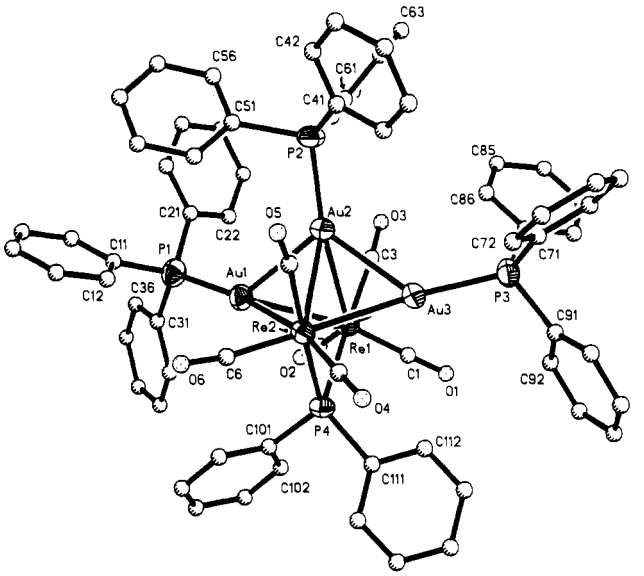

Figure 4. Molecular structure of **7**, showing the atom-numbering scheme (50% tep).

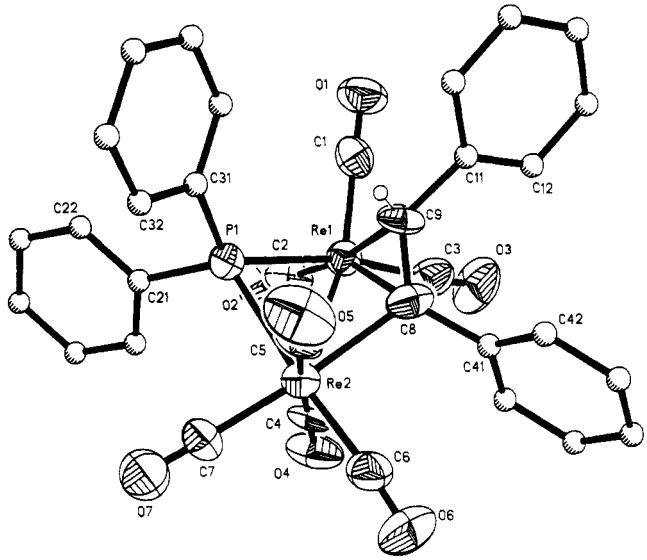

Figure 5. Molecular structure of **8**, showing the atom-numbering scheme (50% tep).

Complex 7. The Re_2Au_3 core in the diamagnetic substance **7** is trigonal bipyramidal and of idealized C_{2v} symmetry (Figure 4). Both Re atoms are bridged by a PPh_2 group. Furthermore each Re atom has three terminal CO ligands, which, in the compounds **4** and **7**, have common geometrical arrangement (C_{3v}) and, as viewed along the Re–Re bond axis, nearly eclipsed conformation. But a valence electron count of 34 is achieved only if a Re–Re double bond is assumed. The Re–Re bond length in **7** is 2.914 (3) Å and shortened by 0.208 (3) Å from that observed in **4**. This bond length in **7** is somewhat longer than values obtained for similar Re–Re double bonds in $[Re_3(\mu_3\text{-}H)_2(\mu\text{-}PPh_2)_3(CO)_6]$ (2.730 (1) Å)[30] and $[Re_3(\mu\text{-}H)_4(CO)_{10}]$ (2.789 (1) Å)[9] but comparable with the values found in $[Re_2(\mu\text{-}H)_2(CO)_8]$ (2.896 (3) Å),[31] $[Re_2(\mu\text{-}H)_2(CO)_6(Ph_2PCH_2PPh_2)]$ (2.893 (2) Å),[32] and

(22) Jeffry, C. J.; Orpen, G. A.; Stone, F. G. A.; Went, M. J. *J. Chem. Soc., Dalton Trans.* **1986**, 173.
(23) Lonato, B.; Norton, J. R.; Huffman, J. C.; Marsella, J. A.; Caulton, K. G. *J. Am. Chem. Soc.* **1981**, *103*, 209.
(24) Fischer, E. O.; Rustemeyer, P.; Neugebauer, D. *Z. Naturforsch., B* **1980**, *35*, 1083.
(25) Jeffery, J. C.; Orpen, A. G.; Robinson, W. T.; Stone, F. G. A.; Went, M. J. *J. Chem. Soc., Chem. Commun.* **1984**, 396.
(26) Blickensdoerfer, J. R.; Kobler, C. B.; Kaesz, H. D. *J. Am. Chem. Soc.* **1975**, *97*, 2686.
(27) Green, M.; Orpen, G. A., Schaverien, C. J.; Williams, J. D. *J. Chem. Soc., Chem. Commun.* **1983**, 1399.
(28) Churchill, M. R.; Amoh, K. N.; Wassermann, H. J. *Inorg. Chem.* **1981**, *20*, 1609.
(29) Sutherland, B. R.; Folting, K.; Streib, W. E.; Ho, D. M.; Huffman, J. C.; Caulton, K. G. *J. Am. Chem. Soc.* **1987**, *109*, 3489.
(30) Haupt, H. J.; Balsaa, P.; Flörke, U. *Angew. Chem., Int. Ed. Engl.* **1988**, *27*, 263.
(31) Bennet, M. J.; Graham, W. A. G.; Hoyano, J. K.; Hutcheon, W. L. *J. Am. Chem. Soc.* **1972**, *94*, 6232.

$[Re_3(\mu\text{-}H)_3(CO)_9(\mu_3\text{-}AuPPh_3)]^-$ (2.889 (1) Å).[9] This metal–metal double-bond assignment in **7** represents an upper limit for such a bond, due perhaps to the greater steric requirement of the bridging gold phosphine. Taking the $Re_2Au(2)$ arrangement in the Re_2Au_3 core of **7** as a basis plane, this is capped by the apical Au(1) and Au(3) atoms. This realizes the coordination number 5 for Au(2) and 4 for the Au(1) and Au(2) atoms, if the phosphorus ligand atom is involved. Their average bond distances are Au(2)–Re = 2.816 (2) Å and Au(1)(3)–Re = 2.835 (2) Å. The values obtained are shorter than the Au–Re length of 2.901 (2) Å in **4**, but they are consistent with that of 2.837 (1) Å in the unsaturated 44-electron triangular species $[Re_3(\mu\text{-}H)_3(CO)_9(\mu_3\text{-}AuPPh_3)^-]$.[9] Finally, the unique metal–metal bond in **7** is the enlarged Au–Au bond (which accompanies the shortened Re–Re bond). The average Au–Au bond length of 2.829 (2) Å is longer than that of 2.734 (2) Å in **4**.

Complex 8. The vinylic PhHC=CPh group of **8** (Figure 5) is π-bonded to Re(1) and σ-bonded to Re(2) via C(8). This $(\mu\text{-}\sigma\text{:}\eta^2\text{-}CPh{=}CHPh)$ ligand does not take up an orientation trans to the phosphido bridge with respect to the midpoint of the Re–Re vector but adopts a cisoid configuration with an angle of 126.2° between the Re(1)–Re(2)–C(8) and Re(1)–Re(2)–P(1) planes. The C(8)–C(9) bond length of 1.394 (16) Å is in accordance with the corresponding value of 1.396 (4) Å in $[Os_3(\mu\text{-}H)(\mu\text{-}\sigma\text{:}\eta^2\text{-}CH{=}CH_2](CO)_{10}$[33] and equivalent to the length of the formal C=C double bond upon coordination to a metal. The second bridging group is PPh_2 with the subtended bond angle at the phosphorus ligand atom of 75.1 (1)°. The acute angle indicates a Re–Re bond. Its value is 2.998 (1) Å and is comparable to that of the single Re–Re bond in $\mathbf{2}^-$ (Re–Re = 3.062 (2) Å). Besides the donor atoms C(8), C(9), and P(1) mentioned, the Re(1) and Re(2) atoms have three and four terminal CO ligands in the coordination sphere. Compound **8** obeys the EAN rule with a 34-electron count.

The Re–C(carbonyl) distances for the axial groups on Re(2) are 1.956 (17) Å (average), Re–C with CO trans to P is 1.951 (17) Å (average), and Re–C with CO trans to C(8) is 1.938 (14) Å. The longer axial Re–C bonds are in accordance with π-acceptor properties of two competing carbonyls. A similar situation exists that is seen for the carbonyl pseudotrans to the vinylic ligand, which explains the similar Re(1)–C(2) value of 1.960 (15) Å. The lowest of such Re–CO values measured is 1.896 (14) Å for the Re(1)–C(1) bond length and is therefore not competing strongly with other ligands for back-donation from a particular metal orbital.

Intramolecular distances in $\mathbf{2}^-$–**4**, **7**, and **8** do not indicate interactions greater than those for van der Waals forces.

Cyclic Voltammetric Measurements. The dinuclear phosphido-bridged substance **1** shows an irreversible oxidation transfer with the maximum at 1.508 V vs NHE. The related half-width of the peak $E_p - E_{p/2}$ indicates a one-electron step. To explain the origin of the transferred electron, a general MO description of such small metal atom cluster compounds is helpful.[34] The HOMO shows bonding M–M character, while the LUMO is M–M antibonding. Consequently, the strength of the Re–Re bond is lowered by a one-electron oxidation, while Re–CO bonds are labilized. Such weakened bonds naturally favor a decomposition that is more rapid than the reverse redox process, as it was observed for a large number of transition-metal carbonyl clusters.[35] Another reason for a missing reversibility of the redox process is the strong chemisorption effect of the working electrode used. For the substance $Fe_2(\mu\text{-}PPh_2)_2(CO)_6$, which is similar to **1**, this was the case at a platinum working electrode, and the effect could be avoided by use of a dropping-mercury electrode.[15] The analogous modification could not be implemented for the measurements of **1** because the dropping-mercury electrode is limited to a range of 700 mV. To clarify the origin of the irreversibility for compound **1** as for other compounds examined, we have done the electrochemical measurements with various solid working electrodes, but the change from a platinum to a gold and finally to a glassy-carbon electrode showed no effect on the value of $E_{p,a1}$. These results support the above-mentioned interpretation of the irreversible redox process.

Table X. Redox Potentials of the Substances **4**–**7** and **9**

	E^f, mV[a]	ΔE, mV[a]	$i_{p,c}/i_{p,a}$	$E_{p,a2}$, mV[a]
4	682	80	0.9	984 (irrev)
5	696	86	0.89	981 (irrev)
6	691	82	1.07	1011 (irrev)
7	289	76	1	
	752	90	0.5	
9	576	78	0.95	863 (irrev)

[a] E vs NHE with v = 50 mV/s.

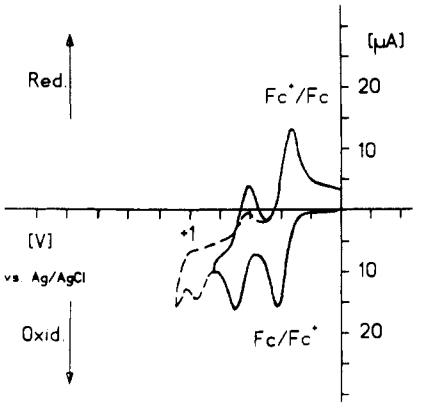

Figure 6. Cyclic voltammogram of **4** (0.50 mmol/L) in CH_2Cl_2 solution on a platinum electrode (v = 0.05 V/s; 0.1 m (TBA)PF_6; c(ferrocene) = 0.5 mmol/L).

For the mixed rhenium–gold clusters the properties of each HOMO in the substances **3**–**7** and **9** must be determined mainly through an overlap between the rhenium orbitals generating the Re–Re bond, on the basis of the first ionization potentials of Re (7.87 eV) and Au (9.22 eV) atoms. Such an assumption demands that a change from electron-poor to electron-rich groups bridging the Re–Re bond in the same type of compounds should give a shift to smaller E^f values, equivalent to a facilitation of the oxidation step of the redox process. This is observed for the E^f values of the metallatetrahedral type complexes $[(\mu\text{-}C(R)O)(\mu\text{-}PPh_2)(CO)_6Re_2(AuPPh_3)_2]$ (Table X). In every case, these show both a reversible and an irreversible oxidative one-electron step (Figure 6). The decrease in E^f value from the electron-poor phenyl acyl (R = Ph) derivative **4** (E^f = 682 mV) to the electron-rich dialkylamido acyl (R = N(i-Pr_2)) derivative **9** (E^f = 576 mV) is 106 mV. This supports the idea that the cyclic voltammetric data for the substances **3**–**7** and **9** measured depend on the electronic property of the substituent pattern attached to the dirhenium fragment.

Other data show that the isolobal exchange of the proton in **1** ($E_{p,a}$ = 1508 mV) by the PH_3Au group in **3** ($E_{p,a}$ = 1132 mV) shifts the oxidative potential of about 376 mV in the cathodic direction. Complex **3** shows an irreversible oxidative electron transfer, and the half-width of the related peak correlates with that of a one-electron transfer. Going from **3** to the substances of metallatetrahedral type **4**–**6** and **9**, this is accompanied formally by an exchange of one CO ligand for an additional $AuPPh_3$ group and the additional conversion of another coordinated CO into a μ-C(R)O group. The first oxidative electron process ($E_{p,a}$) changes from an irreversible process in **3** to reversible ones in **4**–**6** and **9**.

The reversible one-electron redox process of **4** is shown in Figure 6 within the range −1.2 to 0.8 V vs NHE. As it was ascertained

(32) Mays, M. J.; Prest, D. W.; Raithby, P. R. *J. Chem. Soc., Chem. Commun.* **1980**, 171.
(33) Orpen, A. G.; Pippard, D.; Sheldrick, G. M.; Ronse, K. D. *Acta Crystallogr., Sect. B: Struct. Crystallogr. Cryst. Chem.* **1978**, *34*, 2466.
(34) (a) Hall, M. B.; Fenske, R. F.; Dahl, L. F. *Inorg. Chem.* **1975**, *14*, 3103. (b) Fenske, R. F.; Dahl, L. F.; Yon, X. *J. Mol. Sci. (Int. Ed.)* **1986**, *4*, 211 and references cited therein.
(35) Lemoine, P. *Coord. Chem. Rev.* **1988**, *83*, 1696 and references cited therein.

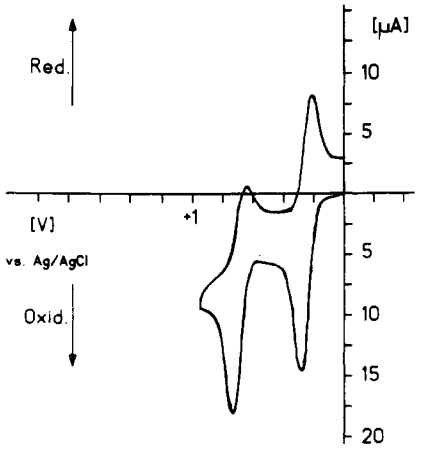

Figure 7. Cyclic voltammogram of **7** (0.58 mmol/L) in CH_2Cl_2 solution on a platinum electrode (v = 0.05 V/s; 0.1 m $(TBA)PF_6$).

Table XI. Oxidation Potentials of the Substances **1–3**

	$E_{p,a1}$, mV[a]	$\lvert E_p - E_{p/2}\rvert$, mV	$E_{p,a2}$, mV	$\lvert E_p - E_{p/2}\rvert$, mV
1	1508 (irrev)	80		
2	241 (irrev)	88	1058 (irrev)	120
3	1132 (irrev)	80		

[a] E vs NHE with v = 50 mV/s.

by separate measurements for **4**, first, the related potential E^f does not depend on the scan velocity and, second, the difference between the oxidative and reductive potential (ΔE) is 80 mV. This value also results under analogous experimental conditions for ferrocene (Fc/Fc^+), which represents an ideal one-electron-transfer system.[36] A further requirement of this system is that $i_{p,c}/i_{p,a}$ = 1 and additionally does not depend on different voltage scans. Whereas the last criterion is exactly fulfilled, a small deviation present is observed, namely $i_{p,a}/i_{p,a}$ = 0.9. In spite of this, it is acceptable to consider this a reversible one-electron transfer.[37] Enlargement of the anodic potential barrier from 0.8 to 1.2 mV vs NHE leads to a second oxidation step ($E_{p,a2}$) that is irreversible, concomitant with loss of the reversibility of the first peak (E^f). Such a 2-fold oxidation of the phenyl acyl bridged substance that removed both electrons from the HOMO might be accompanied by an irreversible fission of the Re–Re bond. The proposed intermediate possibly formed may be obtained by a retrosynthesis of the acyl bridging group under formation of the hypothetical cation $[(\mu\text{-}PPh_2)(CO)_7(Ph)(AuPPh_3)_2Re_2^{2+}]$. This explanation of the process is consistent with a so-called $E_rE_rC_i$ mechanistic pathway.[37,38]

The electrochemical properties of the other acyl derivatives **5**, **6**, and **9** are similar. For example, their E^f values differ less than 10 mV for the compounds **4** (R = Ph), **5** (R = Me), and **6** (R = *n*-Bu).

In the order from the acyl derivatives to substance **7** (Figure 7), the number of reversible redox processes is doubled formally as consequence of a higher metal nuclearity and the release of the acyl bridge. Complex **7** shows the first reversible one-electron-transfer process at 289 mV vs NHE (ΔE_p = 76 mV; $i_{p,c}/i_{p,a}$ = 1) and the second quasi-reversible process at 752 mV vs NHE (ΔE_p = 90 mV; $i_{p,c}/i_{p,a}$ = 0.5). The stabilization effect observed electrochemically is supported through a π-delocalization effect, since only the compound **7** has an Re–Re double bond.

The isoelectronic substances of lower metal nuclearity **1**, **3**, and $\mathbf{2}^-$ show irreversible one-electron-transfer processes (Table XI). Proton substitution by the isolobal $[AuPPh_3^+]$ fragment shifts $E_{p,a1}$ from 1508 mV in **1** to 1132 mV in **3** and subsequently to 241 mV in $\mathbf{2}^-$. The decreasing values in this order suggest an increasing electron-rich Re_2 core in the substances. In the case of the anion $\mathbf{2}^-$ it is proposed that $E_{p,a1}$ is due to the neutral species **2** and that $E_{p,a2}$ at 1058 mV is due to the hypothetical cation $[(\mu\text{-}PPh_2)(CO)_8Re_2]^+$. The reduction of $\mathbf{2}^-$ is not observed until −1.5 V, which is the limiting value of our cyclic voltammetric equipment.

Supplementary Material Available: For $[C_{20}H_{10}O_8PRe_2][C_8H_{20}N]$ ($[C_8H_{20}N][\mathbf{2}]$), $AuC_{38}H_{25}O_8P_2Re_2{\cdot}CH_2Cl_2$ (**3**), $Au_2C_{61}H_{45}O_7P_3Re_2$ (**4**), $Au_3C_{72}H_{55}O_6P_4Re_2{\cdot}2CH_2Cl_2$ (**7**), and $C_{33}H_{21}O_7PRe_2$ (**8**), full tables of crystal data, atomic positional parameters, bond lengths, bond angles, anisotropic displacement parameters, and hydrogen coordinates (22 pages); observed and calculated structure factors (147 pages). Ordering information is given on any current masthead page.

(36) Gagne, R.; Koval, C. A.; Lisensky, G. *Inorg. Chem.* **1980**, *19*, 2854.
(37) Bard, A. J.; Faulkener, L. R. *Electrochemical Methods*; John Wiley & Sons: New York, 1980; Chapter 6, p 451.
(38) Heinze, J. *Angew. Chem.* **1984**, *96*, 823.